Available online at www.sciencedirect.com

ScienceDirect

IFAC PapersOnline CONFERENCE PAPER ARCHIVE

IFAC PapersOnLine 59-6 (2025) 295–300

Model-based protein estimation during dough formation in a Farinograph

A. Schaum [*,**], **S. Tronci, M. Grosso** [***]

[*] *Department of Process Analytics, University of Hohenheim, Stuttgart, Germany*
e-mail: {arthur.lepsien;alexander.schaum}@uni-hohenheim.de
[**] *Computational Science Hub, University of Hohenheim, Stuttgart, Germany*
[***] *Chemical Engineering Department, University of Cagliari, Sardegna, Italy*

Abstract: The problem of estimating the protein content in dough during kneading in a farinograph is addressed exploiting underyling structural observability of a suitable model describing the biochemical reaction network of different protein fractions involved in the formation of the gluten network in the dough and its deterioration due to excessive kneading. Based on an observability analysis for the model a reduced order geometric observer and an extended Kalman Filter are designed and tested with experimental data from dough kneading experiments. The results highlight the potential of incorporating such model-based process analytic tools for improved monitoring of the underlying biochemical mechanisms involved in dough formation, and for providing an additional means for estimation of protein content in flour during standard kneading processes.

Keywords: Dough development, process analytic technology, state estimation.

1. INTRODUCTION

The analysis of flour and its effects on dough preparation, and thus later for baking product quality is a key task in cereal-based food industries. A typical approach for this task is to use so-called farinograph units (see Figure 1) in which a defined amount of water is added to the flour while kneeding with a fixed speed. This analysis tool is very similar to the mixograph test (Martinant et al., 1998). As in the flour in presence of water different kind of biochemical processes start during mixing leading to the formation of three-dimensional network of gluten proteins the viscosity changes over time. The farinograph basically measures the required torque to ensure a constant kneading velocity and thus provides a measure for the dough viscosity.

While typically in food engineering physical and chemical analystic methods, as well as chemometry are well established for flour and dough analysis, the employment of mathematical models lacks relatively far behind (Van Boekel, 2008; Hitzmann et al., 2015). For dough development there exist anyway some important exceptions as, e.g., (Roman-Gutierrez et al., 2002; Belton, 2012; Migliori and Correra, 2013; Hermannseder et al., 2017). In these studies mathematical models were proposed based on the bio-chemical insight into the dough formation process (see, e.g., Belton (1999) for the underlying mechanisms), experimentally validated for different kinds of flours, and the model parameters put in perspective with baking product quality measures using regression techniques. A particular outcome of these analysis is that if the initial protein content is sufficiently well known, a value that can

Fig. 1. Farinograph unit employed at the University of Hohenheim for the experimental part of this study.

be rather well estimated using, e.g., NIR spectrometry and chemometrics (see, e.g., (Ranzan et al., 2014)), the optimal dough development time to reach a desired dough viscosity can be calculated. This potentially opens further interesting options of application in process optimization and decision making for operation and production conditions. The drawback of this idea is at the same time that if there is an error in the initial condition this will provide a potentially larger error in the prediction of the dough

2405-8963 Copyright © 2025 The Authors. This is an open access article under the CC BY-NC-ND license.
Peer review under responsibility of International Federation of Automatic Control.
10.1016/j.ifacol.2025.07.161

development time and other quantities derived therefrom. Besides this consideration an additional question occurs, namely, whether it is possible to estimate the protein content from the measurement of the viscosity, or the torque in a farinograph during the running kneading process.

From other areas of process monitoring and control the problem of unknown initial conditions is typically handled using state estimation schemes, like state observers (Alvarez and Lopez, 1999; Jerono et al., 2021) or stochastic filters (Gelb, 1978; Bastin and Dochain, 1990). These approaches are not yet that well established in the food sector in general, and in cereal processing in particular, as they are in chemical and biochemical process engineering applications (Van Boekel, 2008; Hitzmann et al., 2015). One reason for this is the lack of detailed models with real-time capability and well-established model parameters. The latter issue is central to food engineering, as the raw material is subject to strong variations, e.g., fertilization and climatic conditions (Rekowski et al., 2021; Dier et al., 2022). Here, again, approaches from state and parameter estimation can provide interesting solutions.

Having these considerations as point of departure, in the present study the state estimation problem for dough development during kneading is addressed. For this purpose the model proposed in (Hermannseder et al., 2017) is employed. First, an observability analysis is carried out, focussing on the structural observability. Then a geometric observer and an extended Kalman Filter are designed that take as a measurement the dough viscosity measured in Brabender units in the employed farinograh. Both state estimation schemes show a similar performance when compared using experimental data.

2. DOUGH FORMATION MODEL

Consider the model for dough development as proposed in (Belton, 2012) and extended in (Hermannseder et al., 2017)

$$\dot{x}_1 = -k_1 x_1 \tag{1a}$$
$$\dot{x}_2 = k_1 x_1 - k_2 x_2^2 \tag{1b}$$
$$\dot{x}_3 = k_2 x_2^2 - k_3 x_3^2 \tag{1c}$$
$$\dot{x}_4 = k_3 x_3^2 - k_4 x_4 \tag{1d}$$
$$\dot{x}_5 = k_4 x_4 \tag{1e}$$
$$y = \sum_{k=2}^{5} c_i N_i = \boldsymbol{c}^{\mathrm{T}} \boldsymbol{x} \tag{1f}$$

with x_1 denoting the concentration of proteins in the unhydrated state, x_2 for those in the unstrained state, x_3 for those in the strained state, and x_4, x_5 for those in an intermediate and broken state, respectively. The measurement y corresponds to a measure of viscosity as provided by the farinograph standard and given in Brabender units BU.

In compact notation for later use the system is written as

$$\dot{\boldsymbol{x}} = \boldsymbol{f}(\boldsymbol{x}) \tag{2a}$$
$$y = \boldsymbol{c}^{\mathrm{T}} \boldsymbol{x}. \tag{2b}$$

For the dynamics (1) the following Lemma, which is the manifestation of the underlying mass conservation, is straight forward to prove, but provides important insight for the subsequent analysis.

Lemma 1. For initial condition $\boldsymbol{x}_0$ with $x_{o,i} \geq 0$, $i = 1, \ldots, 5$ the solutions of (1) remain positive, i.e., $0 \leq x_i(t)$ for all $t \geq 0$. Furthermore, it holds that (i) $m(t) = \sum_{i=1}^{5} x_i(t)$ is constant, (ii) $\lim_{t\to\infty} x_i(t) = 0$ for $i = 1, \ldots, 4$, as well as (iii) $\lim_{t\to\infty} x_5(t) = m(0)$.

Proof: Positivity of the solutions can easily be verified by looking at the sign of $\dot{x}_i$ at $x_i = 0$, implying non-negative values at these boundaries of the hyperquadrant $\mathbb{R}_{\geq 0}$. This implies that the vector field everywhere on these boundaries points into the hyperquadrant. Further, it holds that $x_1(t)$ converges to zero exponentially. From the structure of $x_i, i = 2, 3, 4$ the input-to-state stability (Sontag, 1989; Sontag and Wang, 1995) follows with respect to x_{i-1}, implying the input-to-state stability of the whole cascade consisting of x_2 to x_4. Given that $x_1 \to 0$ the exponential asymptotic stability of the cascade system follows. Given that with m as defined in the Lemma it holds that $\dot{m} = 0$ for all $t \geq 0$ one concludes that $\lim_{t\to\infty} x_5(t) = m(0)$ as claimed. □

Based on these properties in the following only the subset of positive states is considered as state space, i.e.,

$$\boldsymbol{x}(t) \in \mathcal{X} := \{\boldsymbol{x} \in \mathbb{R}^n \mid x_i \geq 0,\ i = 1, \ldots, 5\} \subset \mathbb{R}^5. \tag{3}$$

3. STRUCTURAL OBSERVABILITY

In this section the structural observability Lin (1974); Dion et al. (2003); Liu et al. (2012) of the dough development model (1) is analyzed in the understanding that the structural observability is a necessary condition for the local observability and provides an important basis for design of an observer–based process monitoring using state estimation schemes.

Definition 1. The system is structurally observable if it is completely observable for at least one state–parameter pair.

For the analysis of the structural observability the notion of structure graph $\Gamma(\boldsymbol{x}) = (V, E(\boldsymbol{x}))$ of (1) at $\boldsymbol{x} \in X$ is employed. The structure graph consists of the vertex set $V = \{v_1, \ldots, v_5\}$ where v_k is associated to the state x_k, $k = 1, \ldots, 5$, and the directed edge set $E(\boldsymbol{x}) = \{(v_j, v_i) | \frac{\partial f_i(\boldsymbol{x})}{\partial x_j} \neq 0\}$. Note that the edge set in principle depends on the value of $\boldsymbol{x}$, given that $\frac{\partial f_i(\boldsymbol{x})}{\partial x_j}(\boldsymbol{x})$ can become zero in case of vanishing concentration values x_j due to nonlinear reaction rates in (1). The structure graph is extended by introducing the output vertex (see Fig. 2). Concerning the question whether the output of a node contains information on another node can than be answered by moving in the inverse direction of the directed edges. A sufficient condition for the structural observability is then the existence of an information path, i.e., moving in the inverse direction of the edges, from the measured node toward all other nodes without loops.

It should be noted that the so performed structural analysis yields a generic property for a system that depends only on the intrinsic interconnection structure and not on the particular parameter values and the particular state vector

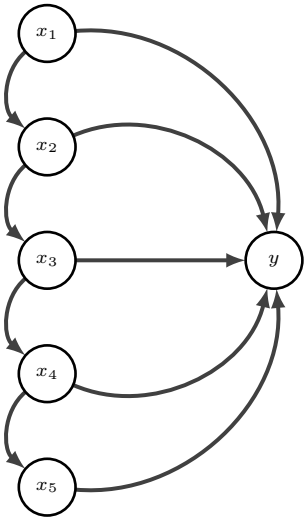

Fig. 2. Structure graph associated to the dough formation model (1).

$\boldsymbol{x}(t) \in \mathcal{X}$ where the partial derivatives are evaluated. It only depends on whether the influence of x_j on x_i is not always zero, thus also allowing for trajectories starting with $x_i(0) = 0$. Indeed, if this relation is not zero for at least one parameter and state, then due to continuity reasons it will be nonzero for almost all values of $\boldsymbol{x}$ and parameters, up to those lying on a specific hyperplane of the state–parameter space with measure zero (cp. (Dion et al., 2003; Liu et al., 2012)).

Based on these notions and the structure graph shown in Figure 2, the following result is obtained.

Theorem 1. System (1) is structurally observable.

Proof: By inspection of the structure graph in Fig. 2 it can be seen that a continuous path exists connecting all nodes starting from y over x_5 to x_1 as long as the directed edges (v_i, v_j) between all state nodes exist. The fact that these connections exist for at least one parameter set and one state vector $\boldsymbol{x}$ follow directly from the model (1). □

Note that given the structural observability, it is in principle possible to estimate all protein concentrations from the torque measurement y. In particular, one can thus estimate the total initial protein content, being the sum m over all protein fractions, which according to Lemma 1 remains constant. The associated problem of state observer or estimator design is addressed in the next section.

4. STATE ESTIMATION

In this section the problem of designing a suitable state estimation scheme to determine the protein content from the measured torque in the farinograph is addressed. For this purpose Lemma 1 is exploited in the sense that the total protein content $m = \sum_{i=1}^{5} x_i$ remains constant over time. Both, a geometric observer exploiting the structure of the model (1) analytically, and an EKF are designed, in order to enable a later comparison.

4.1 Geometric observer

Provided the structure of a reaction chain starting from x_1 and the fact that at the start of the process it holds that $x_i(0) = 0$ for all $i = 2, 3, 4, 5$, it becomes clear that, under the assumption of well identified model parameters, if the first states can be quickly reconstructed, then the remaining states can be predicted correctly. In addition, on the basis of Lemma 1, if the estimation error in the first states converges exponentially to zero, then the remaining estimation errors will converge at least asymptotically. Furthermore, as x_1 does not influence the measurement, it makes sense to focus the correction of an observer on the second state x_2, which directly is reflected in the measured viscosity according to equation (1f).

In consequence to these considerations, in the following a partition of the state vector $\boldsymbol{x}(t)$ into corrected

$$x_o(t) = x_2(t)$$

and uncorrected

$$\boldsymbol{x}_n(t) = [x_1(t),\ x_3(t), x_4(t), x_5(t) - m]^{\mathrm{T}}$$

components is introduced, with m as defined in Lemma 1. The associated dynamics can be written in the following form

$$\dot{x}_o = f_o(x_o, \boldsymbol{x}_n) \tag{4a}$$
$$\dot{\boldsymbol{x}}_n = \boldsymbol{f}_n(x_o, \boldsymbol{x}_n) \tag{4b}$$
$$y = h(x_o, \boldsymbol{x}_n). \tag{4c}$$

Note that with this definition of $\boldsymbol{x}_n$ it follows from Lemma 1 that $\lim_{t\to\infty} [x_o(t)\ \boldsymbol{x}_n(t)] = \boldsymbol{0}$.

Based on this state partition a reduced order geometric observer is proposed with the correction gain $\omega > 0$ in the usual form (see, e.g., (Alvarez and Lopez, 1999; Tronci et al., 2005; Jerono et al., 2021))

$$\dot{\hat{x}}_o = f_o(\hat{x}_o, \hat{\boldsymbol{x}}_n) - \left(\frac{\partial \mathcal{O}}{\partial x_o}(\hat{\boldsymbol{x}})\right)^{-1} \omega\ (h(\hat{x}_o, \hat{\boldsymbol{x}}_n) - y) \tag{5a}$$

$$\dot{\hat{\boldsymbol{x}}}_n = \boldsymbol{f}_n(\hat{x}_o, \hat{\boldsymbol{x}}_n) \tag{5b}$$

with the partial observability map

$$\mathcal{O}(\hat{\boldsymbol{x}}) = h(\hat{x}_o, \hat{\boldsymbol{x}}_n) = c_2 x_2 + \sum_{i \notin \{1,2\}} c_i x_i. \tag{5c}$$

The associated estimation error dynamics can best be analyzed employing the diffeomorphic state transformation

$$\boldsymbol{z} = \boldsymbol{\Phi}(\boldsymbol{x}) := \begin{bmatrix} h(x_0, \boldsymbol{x}_n) \\ \boldsymbol{x}_n \end{bmatrix}, \qquad y = z_1 \tag{6}$$

with dynamics

$$\dot{z}_1 = \varphi_1(\boldsymbol{z}) := \frac{\partial h(\boldsymbol{x})}{\partial \boldsymbol{x}} \boldsymbol{f}(\boldsymbol{x})|_{\boldsymbol{x}=\Phi^{-1}(\boldsymbol{z})} \tag{7}$$

$$\dot{\boldsymbol{x}}_n = \boldsymbol{\varphi}_n(\boldsymbol{z}) := \boldsymbol{f}_n \left(\frac{1}{c_2} \left(z_1 - \sum_{i \notin \{1,2\}} c_i x_i \right), \boldsymbol{x}_n \right). \tag{8}$$

Considering the estimation error in the transformed coordinates, i.e., $\tilde{\boldsymbol{z}} = \hat{\boldsymbol{z}} - \boldsymbol{z}$, it holds that

$$\dot{\tilde{z}}_1 = -\omega \tilde{z}_1 + \tilde{\varphi}_1(\tilde{z}_1, \tilde{\boldsymbol{z}}_n; \boldsymbol{z}) \tag{9a}$$

$$\dot{\tilde{\boldsymbol{x}}}_n = \tilde{\boldsymbol{\varphi}}_n(\tilde{z}_1, \tilde{\boldsymbol{x}}_n; \boldsymbol{z}) \tag{9b}$$

with

$$\tilde{\varphi}_1(\tilde{z}_1, \tilde{\boldsymbol{z}}_n; \boldsymbol{z}) := \varphi_1(\boldsymbol{z} + \tilde{\boldsymbol{z}}) - \varphi_1(\boldsymbol{z}) \tag{9c}$$

$$\tilde{\boldsymbol{\varphi}}_n(\tilde{z}_1, \tilde{\boldsymbol{z}}_n; \boldsymbol{z}) := \boldsymbol{\varphi}_n(\boldsymbol{z} + \tilde{\boldsymbol{z}}) - \boldsymbol{\varphi}_n(\boldsymbol{z}), \tag{9d}$$

with

$$\tilde{\varphi}_i(0, \mathbf{0}; \boldsymbol{z}) = 0 \qquad \forall\ \boldsymbol{z} \in \mathbb{R}^5_{\geq 0}, \quad i = 1, \ldots, 5. \tag{9e}$$

revealing the underlying interconnection structure of the observation error dynamics consisting of two subsystems, associated to $\tilde{z}_1$ and $\tilde{\boldsymbol{x}}_n$, respectively.

Regarding the first subsystem, it holds true that

$$\tilde{z}_1(t) = e^{-\omega t}\left(\tilde{z}_1(0) + \int_0^t e^{\omega\tau}\tilde{\varphi}_1(\tilde{z}_1(\tau), \tilde{\boldsymbol{z}}_n(\tau); \boldsymbol{z}(\tau))\mathrm{d}t\right).$$

Introducing

$$\sigma_1(t) := e^{-\omega t}\left|\tilde{z}_1(0) + \int_0^t e^{\omega\tau}\tilde{\varphi}_1(\tilde{z}_1(\tau), \tilde{\boldsymbol{z}}_n(\tau); \boldsymbol{z}(\tau))\mathrm{d}t\right|$$

From this it follows that

$$|\tilde{z}_1(t)| \leq \sigma_1(t), \quad \forall\ t \geq 0.$$

The dynamics of σ_1 in turn satisfy

$$\dot{\sigma}_1 \leq -\omega\sigma_1 + |\tilde{\varphi}_1(\tilde{z}_1, \tilde{\boldsymbol{z}}_n; \boldsymbol{z})|. \tag{10}$$

In virtue of the mean value theorem (in its differential form) there exists an $0 < \eta < 1$ so that with

$$\boldsymbol{\xi} = \eta\boldsymbol{z} + (1 - \eta)\boldsymbol{\zeta}$$

it holds that

$$\varphi_1(\boldsymbol{z}) - \varphi_1(\boldsymbol{\zeta}) = \nabla\varphi_1(\boldsymbol{\xi})(\boldsymbol{z} - \boldsymbol{\zeta}) \tag{11}$$

$$= \frac{\partial\varphi_1}{\partial z_o}(\boldsymbol{\xi})(z_1 - \zeta_1) + \frac{\partial\varphi_1}{\partial \boldsymbol{z}_n}(\boldsymbol{\xi})(\boldsymbol{z}_n - \boldsymbol{\zeta}_n) \tag{12}$$

implying that at least locally, i.e., over some subset of the state space that basically is a design degree of freedom, there exist constants l_1, l_n so that an upper bound for the above difference can be found as

$$|\varphi_1(\boldsymbol{z}) - \varphi_1(\boldsymbol{\zeta})| \leq l_1|z_1 - \zeta_1| + l_n\|\boldsymbol{z}_n - \boldsymbol{\zeta}_n\|. \tag{13}$$

In consequence it holds that

$$\begin{aligned}\dot{\sigma}_1 &\leq -\omega\sigma_1 + l_1|\tilde{z}_1| + l_n\|\tilde{\boldsymbol{x}}_n\| \\ &\leq -(\omega - l_1)\sigma_1 + l_n\|\tilde{\boldsymbol{x}}_n\|\end{aligned}$$

where the inequality (13) is employed. Using the comparison lemma (Khalil, 1996) this implies the input-to-state stability of $\tilde{z}_1$ with respect to $\tilde{\boldsymbol{x}}_n$ in the case that

$$\omega > l_1. \tag{14}$$

For the second subsystem it holds in virtue of Lema 1 that the corresponding solution $\tilde{\boldsymbol{x}}_n(t) = \tilde{\boldsymbol{\phi}}_n(t, \tilde{z}_1, \tilde{\boldsymbol{z}}_0)$ satisfies for $\tilde{z}_1 = 0$

$$\lim_{t\to\infty}\|\tilde{\boldsymbol{x}}_n(t)\| = \lim_{t\to\infty}\|\tilde{\boldsymbol{\phi}}_n(t, 0, \tilde{\boldsymbol{z}}_0)\| = 0. \tag{15}$$

Note that this property alone is not sufficient for proving the input-to-state stability of the second subsystem with respect to the first one (see, e.g., Sontag and Wang (1995)). In case this property would be ensured one still has to analyze the corresponding small-gain condition to conclude the asymptotic stability of the two-subsystem feedback interconnection (9). This analysis goes beyond the scope of the present paper and instead the convergence behavior is further analyzed for the given experimental setup and compared to an EKF, as outlined in the next section.

Remark 1. One could in principle design a geometric observer with correction in all states, but this would involve the inversion of the observability map, which at points where $x_i(t) \approx 0$ particularly for $i = 2, 3$ will lead to ill-conditioning and lack of numerical robustness, due to the quadratic dependency of the reaction rates on these states.

4.2 Extended Kalman Filter

In addition to the above designed geometric observer a continuous-time extended Kalman Filter (EKF) (Gelb, 1978; Reif et al., 2000) is proposed for comparison. Particular properties of the EKF that are useful here are the facts that (i) the EKF does not explicitely require an inversion of the observability map, and (ii) besides an estimate $\hat{\boldsymbol{x}}(t)$ for the state vector, it provides an explicit estimate for the associated estimation error covariance $P(t)$, under the assumption that $\hat{\boldsymbol{x}}(t) - \boldsymbol{x}(t) \sim \mathcal{N}(\mathbf{0}, P(t))$ as long as $\hat{\boldsymbol{x}}_0 - \boldsymbol{x}_0 \sim \mathcal{N}(\mathbf{0}, P_0)$. Considering process model and measurement uncertainties modeled as Gaussian distributed additive zero mean white noise with covariances Q and R, respectively, the EKF is defined by the the equation set

$$\dot{P} = A^{\mathrm{T}}P + PA + Q - P\boldsymbol{c}R^{-1}\boldsymbol{c}^{\mathrm{T}}P, \tag{16a}$$

$$A = \frac{\partial\boldsymbol{f}}{\partial\boldsymbol{x}}(\hat{\boldsymbol{x}}) \tag{16b}$$

$$\dot{\hat{\boldsymbol{x}}} = \boldsymbol{f}(\hat{\boldsymbol{x}}) - P\boldsymbol{c}R^{-1}\left(\boldsymbol{c}^{\mathrm{T}}\boldsymbol{x} - y\right) \tag{16c}$$

with the associated initial conditions $\hat{\boldsymbol{x}}(0) = \hat{\boldsymbol{x}}_0$ and $P(0) = P_0$. The outcome of the EKF can thus be interpreted as an approximation of the associated state estimation probability density function in form of a Gausian distribution $\mathcal{N}(\hat{\boldsymbol{x}}(t), P(t))$.

This stochastic interpretation of the estimate of the EKF can be particularly useful taking into account different sources of uncertainty in the considered model, e.g., on temperature variations, oxygen increase within the dough and the parallel microbiological mechanisms due to yeast fermentation starting already during kneading providing different products, in particular CO_2.

5. RESULTS

The two state estimation schemes designed above, i.e., the reduced order geometric observer and the EKF have been evaluated with experimental data obtained in a Farinograph AT from Brabender (now Anton Paar) using flour of type Bussard following standard procedures for determining the amount of water added to the flour before kneading. The experiment was carried out three times and the resulting mean value is used for the subsequent analysis. The model parameters have been slightly adapted from (Hermannseder et al., 2017) employing `fmincon` in MATLAB for parameter optimization. The resulting parameters are listed in Table 1. Note that the for parameter estimation the initial value for unhydrated protein content $x_{1,0} = 13.4$ was used, which was determined separately using total protein content analysis of the flour.

The geometric observer and the EKF have been implemented in MATLAB and solved with `ode45`. For this purpose the experimental data have been interpolated at the evaluation time steps of the solver using `interp1`.

The initial condition of the simulation model without correction, the geometric state observer (with $\omega = 10$)

Table 1. Parameters for the dough formation model (1) and initial conditions.

Parameter	value
k_1	0.0471
k_2	0.0120
k_3	0.0089
k_4	0.0006
c_2	29.2865
c_3	0.0019
c_4	42.5505
c_5	25.2435
$x_{1,0}$	13.4
$\hat{x}_{1,0}$	5

and the EKF were set erronously to validate the correction mechanisms of the two state estimation schemes. For this purpose the value of $\hat{x}_{1,0} = 5$ was used, leading to an underestimation of the resulting viscosity, measured here by the torque of the kneading unit. This can be seen in Fig. 3, showing the experimental value with triangles and the model-based simulation with erronous initial condition with a dotted line.

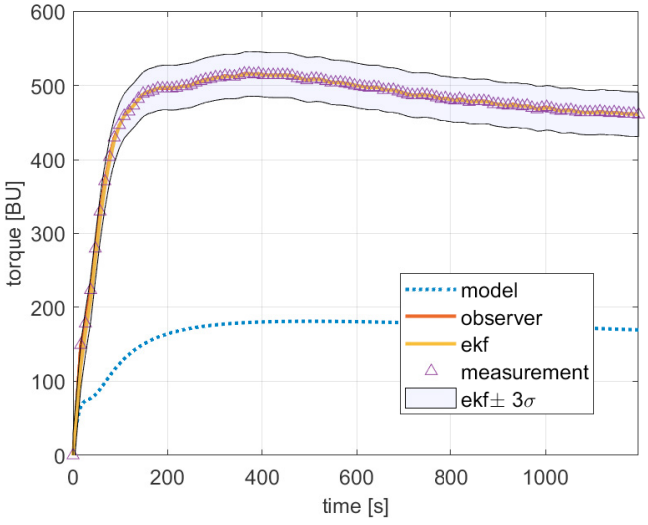

Fig. 3. Torque evolution (in BU) for the experiment with measurement (triangles), model simulation (dotted line), reconstruction from the reduced order geometric observer (red continuous line), the EKF (yellow continuous line) and its $\pm 3\sigma$ certainty interval.

The resulting predictions of the measurement using the geometric state observer and the EKF are also shown in Fig 3, with the geometric observer prediction in red and the EKF in yellow. It can be appreciated that almost no difference is visible between both methods regarding the measurement. In addition to the estimated value the $\pm 3\sigma$ certainty interval evolution of the EKF is included, where σ is calculated using the estimation error covariance matrix P calculated by the EKF according to (16) as

$$\sigma = \sum_{i=2}^{5} c_i \sigma_{ii}, \qquad \sigma_{ii}^2 = P_{ii}, \quad i = 1, \dots, 5. \tag{17}$$

In addition to the comparison regarding the experimental measurement, the state evolutions of the protein fractions $x_1, \dots, x_5$ are shown in Fig. 4. The model simulation without correction is shown as dotted lines, the state estimates of the reduced order geometric observer by the red lines and the ones of the EKF by the yellow lines, together with the related $\pm 3\sigma_{ii}$ certainty intervals. It can be seen from the figure that different state estimates are obtained using the EKF and the geometric observer, due to the different form of measurement injection, which for the geometric observer only introduces a correction of the second state variable $\hat{x}_2$. The final value of the total protein content m (see Lemma 1) obtained with the geometric observer was $\hat{m} = 13.5$, with the actual one determined using offline analysis given by $x_1(0) = 13.4$. The EKF actually provided the same estimate of the total protein content.

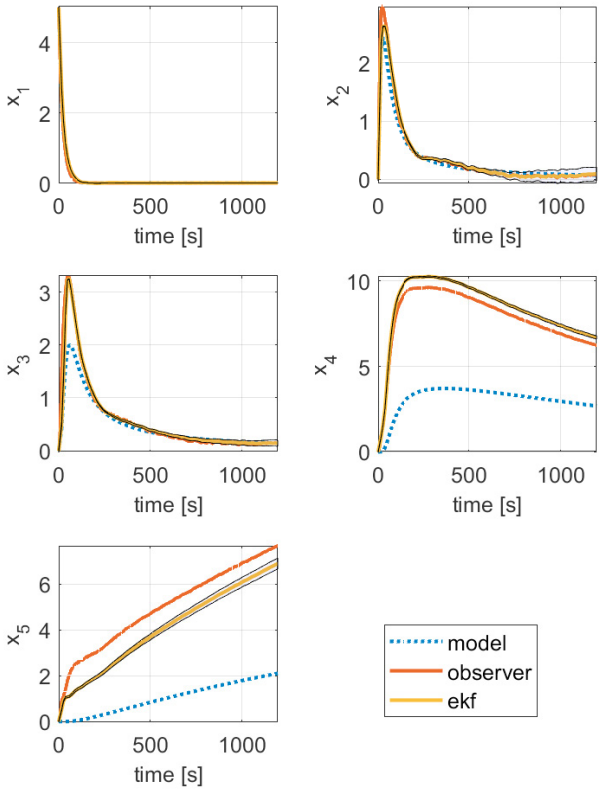

Fig. 4. State evolution of the model simulation (dotted), the reduced order geometric state observer (red) and the EKF (yellow) with $\pm 3\sigma_i$, $i = 1, \dots, 5$ certainty interval for the evaluation with experimental data.

6. CONCLUSIONS

Using a model that has been previously proposed in the literature to describe the change of viscosity during dough kneading, measured through the necessary torque to ensure constant kneading speed, in dependence of the concentration of different protein fractions, from unhydrated to hydrated, strained and broken, it is shown that such protein concentrations can be effectively estimated employing and adapting typical state estimation schemes. For this purpose, first the structural observability of the considered model is established, exploring the intrinsic

reaction mechanisms yielding information content in the measurement signal. Then a geometric observer and an EKF are designed and tested using experimental data obtained with a farinograph. The study thus showcases the potential of using model-based analysis and monitoring tools in cereal processing in particular, and food engineering in general.

Having the contributions of the present study as points of departure, future studies should further exploit the model considered here to improve the convergence results, and evaluate its usefulness in predicting the outcome of dough kneading experiments, in particular the rheological properties by additionally measuring dough viscosity separately, e.g., using a rheometer. Adaptations and extensions of the considered model should therefore be considered as well, and the results of the present study extended accordingly.

REFERENCES

Agrachev, A.A., Morse, A.S., Sontag, E.D., Sussmann, H.J., Utkin, V.I., and Sontag, E.D. (2008). Input to state stability: Basic concepts and results. Nonlinear and optimal control theory: lectures given at the CIME summer school held in Cetraro, Italy June 19–29, 2004, 163–220.

Alvarez, J. and Lopez, T. (1999). Robust dynamic state estimation of nonlinear plants. AIChE Journal, 45 (1), 107–123.

Bastin, G. and Dochain, D. (1990). On-line estimation and adaptive control of bioreactors. Elsevier, Amsterdam.

Belton, P.S. (2012). The molecular basis of dough rheology.

Belton, P. (1999). Mini review: on the elasticity of wheat gluten. Journal of cereal science, 29(2), 103–107.

Dier, M., Hüsken, A., Mikolajewski, S., Langenkämper, G., and Zörb, C. (2022). Analyzing a saturation effect of nitrogen fertilization on baking volume and grain protein concentration in wheat. Agriculture, 13(1), 20.

Dion, J., Dommault, C., and van der Woude, J. (2003). Generic properties and control of linear structured systems: a survey. Automatica, 39, 1125–1144.

Gelb, A. (1978). Applied Optimal Estimation. M.I.T. Press, Cambridge.

Hermannseder, B., Ahmad, M.H., Kügler, P., and Hitzmann, B. (2017). Prediction of baking results from farinograph measurements by using stepwise linear regression and artificial neuronal networks. Journal of Cereal Science, 76, 64–68.

Hitzmann, B., Hauselmann, R., Niemoeller, A., Sangi, D., Traenkle, J., and Glassey, J. (2015). Process analytical technologies in food industry-challenges and benefits: a status report and recommendations. Biotechnology Journal.

Jerono, P., Schaum, A., and Meurer, T. (2021). Observability analysis and robust observer design for a continuous yeast culture. Journal of Process Control, 104, 62–73. doi:https://doi.org/10.1016/j.jprocont.2021.05.012.

Khalil, H. (1996). Nonlinear Systems. Prentice-Hall, Upper Saddle River, New Jersey, 2nd edition.

Lin, C.T. (1974). Structural controllability. IEEE Trans. Autom. Control., 19, 201–208.

Liu, Y., Slotine, J., and Barabasi, A. (2012). Observability of complex systems. Proc. Natl. Acad. Sci., 110, 2460–2465.

Martinant, J., Nicolas, Y., Bouguennec, A., Popineau, Y., Saulnier, L., and Branlard, G. (1998). Relationships between mixograph parameters and indices of wheat grain quality. Journal of Cereal Science, 27(2), 179–189.

Migliori, M. and Correra, S. (2013). Modelling of dough formation process and structure evolution during farinograph test. International journal of food science & technology, 48(1), 121–127.

Ranzan, C., Strohm, A., Ranzan, L., Trierweiler, L.F., Hitzmann, B., and Trierweiler, J.O. (2014). Wheat flour characterization using nir and spectral filter based on ant colony optimization. Chemometrics and intelligent laboratory systems, 132, 133–140.

Reif, K., Gunther, S., Yaz, E.E., and Unbehauen, R. (2000). Stochastic stability of the continuous-time extended kalman filter. IET Control Theory and Applications.

Rekowski, A., Wimmer, M.A., Tahmasebi, S., Dier, M., Kalmbach, S., Hitzmann, B., and Zörb, C. (2021). Drought stress during anthesis alters grain protein composition and improves bread quality in field-grown iranian and german wheat genotypes. Applied Sciences, 11(21), 9782.

Roman-Gutierrez, A., Guilbert, S., and Cuq, B. (2002). Distribution of water between wheat flour components: A dynamic water vapour adsorption study. Journal of Cereal Science, 36(3), 347–355.

Sontag, E.D. (1989). Smooth stabilization implies coprime factorization. IEEE Trans. Autom. Control, 34(4), 435–443.

Sontag, E.D. and Wang, Y. (1995). On characterizations of the input-to-state stability property. Systems & Control Letters, 24 (5).

Tronci, S., Bezzo, F., Barolo, M., and Baratti, R. (2005). Geometric observer for a distillation column: Development and experimental testing. Ind. Eng. Chem. Res., 44, 9884 – 9893.

Van Boekel, M.A. (2008). Kinetic modeling of food quality: a critical review. Comprehensive reviews in food science and food safety, 7(1), 144–158.